Ecological Modelling 510 (2025) 111329

Contents lists available at ScienceDirect

Ecological Modelling

journal homepage: www.elsevier.com/locate/ecolmodel

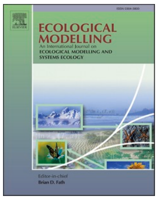

Integrating interspecific traits into biophysical models of seagrass dispersal

Douchan Hanuise [a,c,*], Thomas Dobbelaere [a], Severine Choukroun [c], Michael A. Rasheed [b,c], Jonathan Lambrechts [d], Paul H. York [b], Timothy M. Smith [b], Robert G. Coles [b], Emmanuel Hanert [a,d], Alana Grech [c]

[a] Earth and Life Institute, UCLouvain, Louvain-la-Neuve, Belgium
[b] Centre for Topical Water and Aquatic Ecosystem Research, James Cook University, Cairns, QLD 4870, Australia
[c] College of Science and Engineering, James Cook University, Townsville, QLD 4811, Australia
[d] Institute of Mechanics, Materials and Civil Engineering, UCLouvain, Louvain-la-Neuve, Belgium

ARTICLE INFO

Keywords:
Seagrasses
Great barrier reef
Dispersal
Particle-tracker model
Seagrass vegetative fragments
Coastal ecosystems
Coastal management

ABSTRACT

The resilience of seagrass meadows strongly depends on the dispersal of their propagules, which fosters recovery and replenishment after disturbances. However, predicting dispersal patterns across dynamic coastal environments and large spatial and temporal scales remains challenging due to the lack of empirical observations. Biophysical models, integrating oceanic and atmospheric drivers with species-specific traits such as buoyancy and lifespan, are commonly used to simulate propagule transport. Yet, few studies account for the interspecific and interannual variability inherent in tropical seagrass ecosystems. Here we present a high-resolution seagrass biophysical dispersal model applied to 11 tropical seagrass species across the entire Great Barrier Reef World Heritage Area (GBRWHA), Australia, and run this model over a 6-year period (2011–2016). We use this model to assess how the interspecific variability in the buoyancy and windage of seagrass propagules affect their dispersal patterns and how these patterns further vary both seasonally and interannually. Our results reveal that species-specific factors such as their windage and buoyancy, as well as the season and region in which they disperse had the largest influence on dispersal distance. *H. spinulosa* and *S. isoetifolium* showed the greatest dispersal in the Whitsunday region, while the wet season promoted higher local retention due to lower wind speeds. From a management perspective, this highlights the need to account for species-specific information when devising seagrass management strategies. The outcomes of this research reveal the inherent complexities of predicting multi-species dispersal over large spatial and temporal scales, with broader implications for predicting dispersal in complex coastal ecosystems.

1. Introduction

Marine dispersal plays a critical role in shaping the distribution and resilience of populations, influencing genetic connectivity, species interactions, and ecosystem dynamics (Álvarez-Noriega et al., 2020; Cowen and Sponaugle, 2009; Kendrick et al., 2017; McMahon et al., 2014; Ramirez-Romero et al., 2023). Dispersal is driven by physical forcings such as ocean currents, wind and tidal flows. They can either support (re)colonization and recovery, or hinder the transport of propagules (i.e. seeds, fruits, larvae). Climate change is expected to change dispersal pathways by disrupting ocean circulation, increasing storm frequency, and modifying temperature regimes (Corte et al., 2018; Dobbelaere et al., 2024; Figueiredo et al., 2022; van Gennip et al., 2017; Wilson et al., 2016), which in turn influence larval development and survival (Brown, 2014; Peniston et al., 2024; Tesson and Edelaar, 2013). As environmental conditions continue to change, advancing our understanding of the biological and physical mechanisms underpinning dispersal is both challenging and essential (Lett et al., 2010; Travis et al., 2013; Urban et al., 2016).

Biophysical models offer a feasible method to improve our understanding of complex processes of marine dispersal (Jahnke and Jonsson, 2022; Kendrick et al., 2017). Dispersal biophysical models use a hydrodynamic simulation that estimates current directions and velocities, which can then be used in a particle-tracking model. Some of these models include biological variables, such as decay rate, lifespan, and sometimes buoyancy duration (Kuusemäe et al., 2018; Lai et al., 2024).

---

* Corresponding author at: College of Science and Engineering, James Cook University, Townsville, Queensland, Australia.
E-mail address: douchan.hanuise@my.jcu.edu.au (D. Hanuise).

https://doi.org/10.1016/j.ecolmodel.2025.111329
Received 23 June 2025; Received in revised form 25 August 2025; Accepted 27 August 2025

Model outputs are individuals' dispersal trajectories over space and time. These trajectories would be impossible to estimate empirically due to the small size and large number of propagules, and the difficulty of tracking them continuously over broad spatial and temporal scales. By computing metrics such as dispersal distances, local retention, and connectivity matrices, these trajectories can be used to inform connectivity between populations (Jackson et al., 2021; Lai et al., 2024; Pastor et al., 2023; Ruocco et al., 2025), long distance dispersal potential (Ruiz-Montoya et al., 2015; Smith et al., 2018) and dispersal barriers (Evans et al., 2021; Jahnke et al., 2020). Despite their increasing use, most dispersal biophysical models used a simple biological behaviour to describe dispersal movement of propagules (Swearer et al., 2019).

To date, dispersal biophysical models have rarely been implemented for multi-species habitats, such as tropical seagrass meadows. These models are often simple, focusing on single species over short periods of time, and small spatial scales (Grech et al., 2018, 2016; Jackson et al., 2021). The dispersal behaviour applied in different studies varies considerably, as shown by the wide range of windage values used, defined as the percentage of wind speed contributing to the movement of seagrass vegetative fragments, ranging from 0.9 % (Lai et al., 2024) to 2 % (Grech et al., 2016). These values are even lower when considering flume tank studies, ranging from 0.21 % to 1.393 % (Lai et al., 2020; Tol et al., 2024). Schlaefer et al. (2022) showed the importance of refining windage coefficients to better represent dispersal variations using a sensitivity analysis (Schlaefer et al., 2022). For now, only one biophysical modelling study includes such complex behaviour for tropical seagrass fragments dispersal (Lai et al., 2024). This model focused on a relatively small spatial (1000–1500 km^2) and temporal scales (6-month). While physical parameters like windage have been partially addressed, biological traits, such as species-specific buoyancy duration and survival, remain underrepresented in current dispersal biophysical models.

Species-specific traits are particularly important for tropical seagrass systems, which are dynamic, diverse and occur in multi-species meadows (Collier et al., 2020; Kilminster et al., 2015; Lin et al., 2024). Seagrass meadows in the Great Barrier Reef (GBR) exemplify this complexity, containing 23 % of worldwide seagrass species diversity (Brodie and Waterhouse, 2012), and providing essential ecosystem services, including biodiversity interactions, water quality and carbon sequestration (Brodie et al., 2020; de los Santos, Olivé, et al., 2020; De los Santos, Scott, et al., 2020). Long-distance dispersal is one of several recovery strategies developed by seagrasses in response to the local threats including water turbidity and urban/port development (Grech et al., 2012; McMahon et al., 2014). Dispersal processes in the GBR are driven by winds, tides, and large-scale currents coming from the Coral Sea, along with the influence of coral reef structures, river discharges, and irregular coastline features (Lambrechts et al., 2008; Saint-Amand, Lambrechts, Thomas, et al., 2023). These patterns are modulated by climatic variables, especially the El Niño Southern Oscillation (ENSO), which contributes to interannual shifts in ocean conditions through rainfall and cyclone events (Cai et al., 2021; Chand et al., 2017; Gurdek-Bas et al., 2022).

The goal of this study is to develop new methods for predicting the dispersal of multiple seagrass species in a complex and large coastal environment over a long time period. We simulated ocean circulation for a 6-year period over the entire GBR and implemented a *Multiple species* particle-tracker model including a complex biophysical parameter (i.e. species-specific windage and life-history traits). Hydrodynamic simulations were performed at a fine spatial resolution over the complex reef topography and coastal seascapes. The high-resolution simulation, the time and spatial scales considered, and the bio-complexity in the model allowed us to investigate long distance dispersal in the GBR by resolving the following questions: (1) how does windage influence dispersal distance for different species?; (2) how does seagrass dispersal vary by species morphology and life-history traits, region, season and years?; and (3) what physical and biological factors influence the long dispersal of seagrass in the Great Barrier Reef? This knowledge will improve our understanding of dispersal over broader spatial and temporal scales thus providing information on an important mechanism for seagrass recovery and management.

2. Methods

2.1. Study area and species

The Great Barrier Reef World Heritage Area (GBRWHA) (Fig. 1A) is the largest coral reef ecosystem in the world (Brodie and Waterhouse, 2012; Day and Dobbs, 2013). While famous for its coral, the GBRWHA is also home to one of the most extensive and diverse seagrass ecosystems in the world (Coles et al., 2015; McKenzie et al., 2022). The tropical climate of the region is divided into two main wind patterns: windy (April-September) and not windy season (October-March). The not windy season, mostly corresponding to the tropical wet season, is characterized by weaker and more variable winds, with an increased likelihood of rain and tropical cyclones. In contrast, the windy season (tropical dry season) features coherent south-easterly trade winds, bringing more stable and drier conditions (Choukroun et al., 2010; Huang et al., 2024).

We divided the study area into six regions to support result interpretation: Cape York, Wet Tropics, Burdekin, Mackay and Whitsunday, Fitzroy and Burnett-Mary (Fig. 1A). These regions are designated Natural Resource Management (NRM) areas where local organizations coordinate sustainable management of natural resources including land, water and biodiversity, in partnership with communities and government. This regional subdivision reflects key biogeographic and climatic boundaries along the GBR coast, gathering similar ecosystems, biomes and river systems together, therefore influencing differently coastal ecosystems.

Seagrass monitoring occurs every year in the GBR, as part of the Great Barrier Reef Marine Monitoring Program (MMP) and other monitoring programs focused in areas of high anthropogenic risk (Coles et al., 2015; McKenzie et al., 2023). We did not consider the deep-water habitats here because of their structure complexity and highly variable presence/absence in the GBR (York et al., 2015). We focused on 11 species that occur in inter-tidal and sub-tidal habitats (representing 4925 km^2) along the GBR coast: *Halophila ovalis, Halophila capricorni, Halophila decipiens, Halophila minor, Halophila tricostata, Halophila spinulosa, Syrringodium isoetifolium, Zostera muelleri, Halodule uninervis, Cymodocea rotundata,* and *Cymodocea serrulata.*

To delineate the presence of seagrass in the GBR, we used seagrass spatial distribution data from Carter et al. (2021) (Fig. 1A). The spatial data of Carter et al. (2021) were collated from literature and unpublished monitoring datasets over a 35-year period (1984–2018) (Carter, McKenna, et al., 2021). All data are standardized to a unique shapefile layer containing survey date, method for data collection (boat, diver, helicopter), and seagrass meadow attributes (percentage cover, surface area, dominant species, species present, density, mean biomass). Some of these polygons are therefore 30 to 40 years old and may no longer exist, or new meadows may have developed between the time the data was collected and now. However, this seagrass distribution represents the best available information on potential meadow area, either representing existing meadows or suitable areas for re-establishment. Therefore, by using this layer in the biophysical model, we can capture the full potential of seagrass habitat dispersal in the GBR.

To inform the biological parameters of the biophysical model, we classified the eleven species into six groups based on their leaf morphology: paddle, fern, spaghetti, ribbon thin, ribbon thick long and ribbon thick short (Table 1). Our assumption was that leaf shape and size is the primary influencer of fragment dispersal behaviour (i.e. windage, buoyancy). The smallest group is *S. isoetifolium* (spaghetti leaves species, G3), as this species were recorded dominant in five meadows in the GBR. The largest group was paddle leaf seagrasses (G1), with a very high

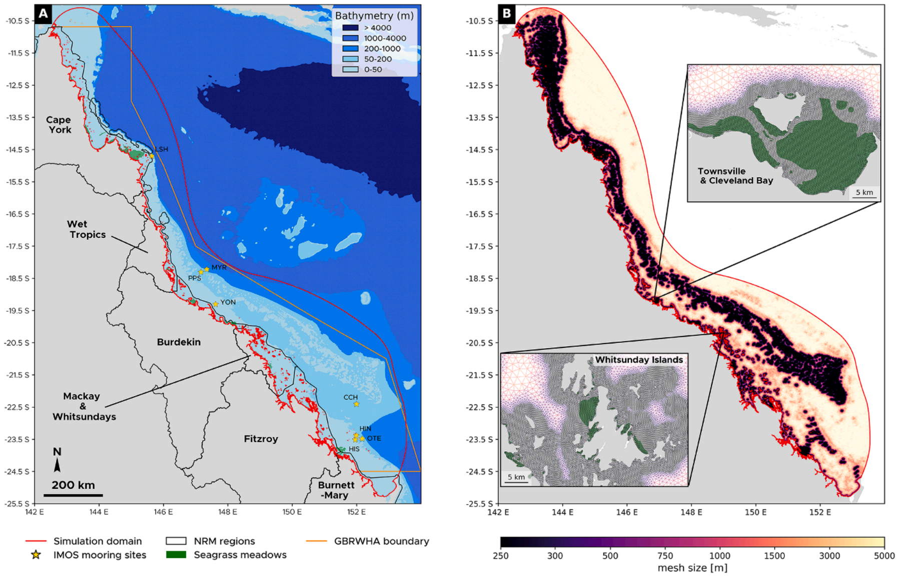

Fig. 1. Overview of the studied area. A: The boundary of the SLIM hydrodynamic model of the GBR (red line) and the boundary of the Great Barrier Reef World Heritage Area (GBRWHA – orange line). Bathymetry of the area is shown with a non-linear scale (blue colours). Green patches represent the seagrass meadows layer used for the simulations - from Carter et al. (2021). Black lines represent the boundaries of the Natural Resource Management units of Queensland, Australia, adjacent to the GBR. IMOS mooring sites used in model validation are shown with a yellow star. B: Mesh used in the SLIM model. Its variable resolution is shown with a purple to yellow gradient (from 250 m to 5 km). The resolution of the mesh is smaller in complex reef and coastal seascapes. The inset map shows two zoomed-in sections of the mesh, overlayed with the seagrass polygon layer (green).

Table 1
Classification of GBR species according to leaf morphology. This classification has been used to developed six different fragment dispersal simulation scenarios.

/	Group 1	Group 2	Group 3	Group 4	Group 5	Group 6
Leaf shape	Paddle	Fern	Spaghetti	Ribbon thin	Ribbon thick long	Ribbon thick short
Species considered	*Halophila ovalis, Halophila capricorni, Halophila decipiens, Halophila minor, Halophila tricostata*	*Halophila spinulosa*	*Syringodium isoetifolium*	*Zostera muelleri, Halodule uninervis*	*Halodule uninervis, Zostera muelleri, Cymodocea rotundata*	*Cymodocea serrulata*
Leaf length from *Flora of Australia**	1–1.45 cm	0.5–20 cm	Up to 30 cm	10 cm x 0.2 cm	0–50 cm x 0.1–0.5 cm	5–30 cm x 0.5–2 cm
Number of meadows where species is dominant (from Carter et al. (2021))	304	78	5	630	641	62
Total area (km^2) – from Carter et al. (2021)	2596.86	496.31	180.12	1023.09	1029.52	622.23
Max buoyancy duration (days)	28	70	49	56	56	56
Reference(s) for max buoyancy duration	(Duarte, 1991; Lai et al., 2020; Weatherall et al., 2016)	(Duarte, 1991; Weatherall et al., 2016)	(Duarte, 1991)	(Duarte, 1991; Evans et al., 2021; Jackson et al., 2021)	(Duarte, 1991; Evans et al., 2021; Jackson et al., 2021)	Unavailable, defined by seagrass experts
Windage	0.21–1.175 %	0.5–1.5 %	1–2 %	0.34–0.96 %	0.5–1.5 %	0.881–1.313 %
Reference(s) for windage values	(Lai et al., 2020; Tol et al., 2024)	Unavailable, defined by seagrass experts	Unavailable, defined by seagrass experts	(Lai et al., 2020; Tol et al., 2024)	Unavailable, defined by seagrass experts	(Lai et al., 2020)

*https://profiles.ala.org.au/opus/foa.

abundance (2596 km^2), comprising mostly *Halophila* species. Some species in the GBR exhibit distinct morphological forms; for example, *H. uninervis* and *Z. muelleri* can display markedly different leaf lengths and widths (Lin et al., 2024; Wagey, 2015; Waycott et al., 2004). To reflect this variation, we divided these species into two groups: one group representing the thin leaf version and the other the thick leaf version of the species (G4 and G5, respectively). Although they are the same species, these forms differ functionally, and we therefore applied different dispersal behaviours (i.e. windage, decay rate and sinking rate) in the model (Fig. 2 and Table 2).

2.2. Hydrodynamics

GBR ocean circulation was simulated using the multiscale coastal ocean model SLIM.[1] The SLIM model has already been applied and validated in the GBR at different scales (Critchell et al., 2015; Lambrechts et al., 2008; Saint-Amand, Lambrechts, and Hanert, 2023). Here we developed a new model setup to cover the entire GBR study area (Fig. 1), with a particular focus on complex coastal areas that are the habitat for seagrasses. We used the 2D barotropic version of SLIM for this case-study because the coastal region of the GBR is considered to be

---

[1] https://www.slim-ocean.be/

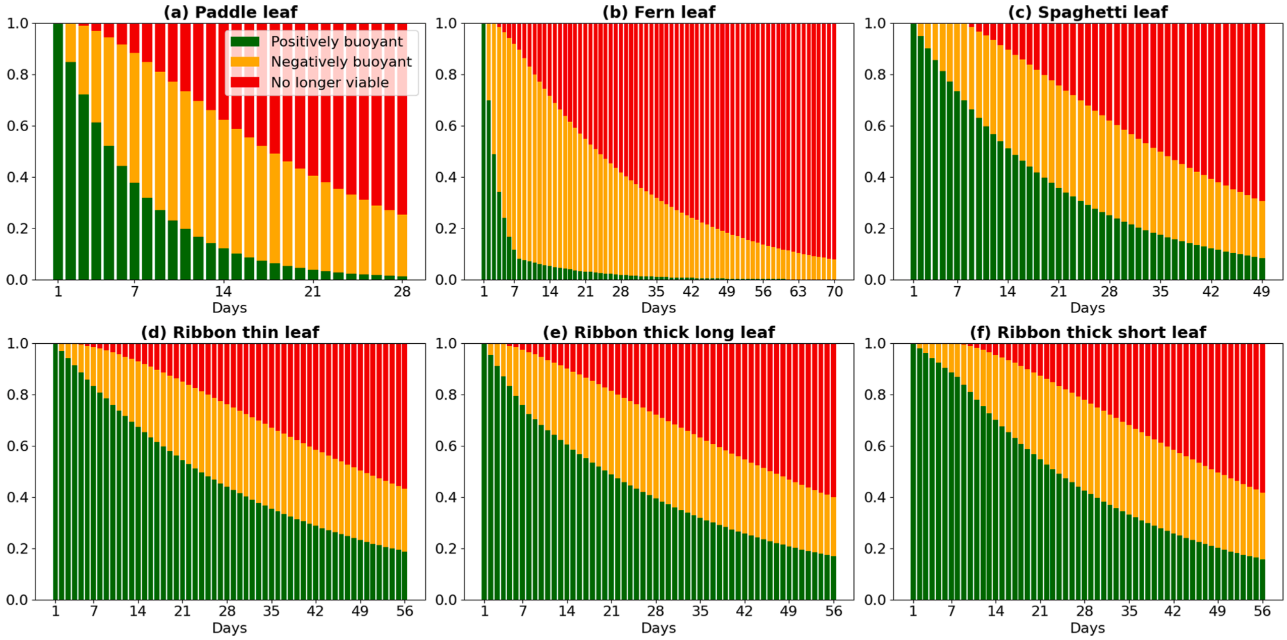

Fig. 2. Biological behaviour implemented in the Lagrangian Particle Tracker for the six different species groups based on leaf morphology. Vertical axis is expressed as the portion of particles, with 1 being 100 % of particles.

Table 2
Species-specific rates used for the transition (day^{-1}) between the three states of life defined in the dispersal model (positively buoyant, negatively buoyant and no longer viable). Different coefficients were established for the first week of dispersal and after the first week of dispersal.

/	G1	G2	G3	G4	G5	G6
"No longer viable" starts after (days)	1	2	10	2	2	10
Sinking rate on the first week (positively buoyant → negatively buoyant)	0.15	0.3	0.05	0.03	0.045	0.02
Decay rate on the first week (negatively buoyant → no longer viable)	0.07	0.03	0.05	0.04	0.045	0.02
Sinking rate after the first week (positively buoyant → negatively buoyant)	0.15	0.07	0.05	0.03	0.03	0.035
Decay rate after the first week (negatively buoyant → no longer viable)	0.07	0.04	0.05	0.04	0.04	0.04

well-mixed (Grech et al., 2016; Luick et al., 2007). The unstructured mesh allows us to refine the spatial resolution of the model in areas with more complex topography. The resolution was set to 250 m over seagrass meadows, coral reefs and near coastlines, and coarsened up to 5 km in more homogenous areas such as the deep sea (Fig. 1B).

The model simulates the sea surface elevation η and the depth-averaged current velocity $\boldsymbol{u}$ by solving the non-linear shallow water equations:

$$\frac{\partial \eta}{\partial t} + \nabla \bullet (H\boldsymbol{u}) = 0, \tag{1}$$

$$\frac{\partial u}{\partial t} + u \bullet \nabla u + f\boldsymbol{e}_z \times u = -g\nabla\eta + \frac{\boldsymbol{\tau}}{\rho H} + D, \tag{2}$$

where $H = h + \eta$ is the water column height, h is the bathymetry, f is the Coriolis parameter, $\boldsymbol{e}_z$ is a unit vector pointing vertically upwards, g is the gravitational acceleration. The bathymetry h is derived from a high-resolution model by the Australian Government, with a 30 m resolution (Beaman, 2017). To ensure that the entire domain is under water during the whole simulation, the minimum depth is set to $h = 3$m. Wetting and drying processes are not considered for this case. The second-last term in Eq. (2) accounts for the effect of wind on water motion and follows the parametrization described in (Smith and Banke, 1975). In this term, τ represents the surface wind stress and ρ is the water density. The wind velocity data are computed by the model ACCESS[2] and made available through eReefs datasets.[3] Finally, $\boldsymbol{D}$ includes the momentum dissipation terms, and is expressed as follows:

$$D = \frac{1}{H}\nabla \bullet [H\nu(\nabla \boldsymbol{u})] - \frac{C_d \| \boldsymbol{u} \| \boldsymbol{u}}{H} \tag{3}$$

The first term is the momentum diffusion with a Smagorinsky non-linear viscosity ν (Smagorinsky, 1963). The second term accounts for the bottom friction. The bulk drag coefficient C_d was set to 2.5×10^{-3} and multiplied by 20 over coral reefs and seagrass meadows to account for the increased roughness of the surface of these ecosystems (Monismith, 2007; Monismith et al., 2019).

On the open boundaries, the exchanges with the Coral Sea are included in the model by forcing it with the sea surface elevation and velocity fields from the GFDL Modular Ocean Model (MOM4),[4] with a 1/10° resolution. Outputs were available through the Bluelink ReANalysis (BRAN2020).[5] The tidal signal, constructed from TPXO9.v5 (Egbert and Erofeeva, 2002), was imposed on the open boundaries. Eqs. (1,2) were solved from January 1st 2011 to January 1st 2018, with a spin-up period of 5 days.

2.3. Model evaluation

We simulated the hydrodynamic of the entire GBR over a 7-year period, from 2011 to 2017. Simulation results were validated against current direction and magnitude data from the IMOS[6] mooring stations (Fig. 1A). This mooring network is constituted by 10 different stations

---

[2] http://www.bom.gov.au/nwp/doc/access/NWPData.shtml
[3] https://research.csiro.au/ereefs/
[4] https://research.csiro.au/bluelink/global/reanalysis/global-model/
[5] https://research.csiro.au/bluelink/bran2020-data-released/
[6] Integrated Marine Observing System (https://portal.aodn.org.au/)

widespread along the GBR coast. Current and tidal observations were not available during all the simulated period (2011–2017) at all stations. As a result, eight stations were mainly used to validate the model: Palm Passage (PPS); Myrmidon Reef Slope (MYR); Yongola (YON); Capricorn Channel (CCH); One Tree East (OTE); Heron Island South (HIS); Heron Island North (HIN) and Lizard Island Shelf (LSH) (Fig. 1 and supplementary materials – Fig. S1-S9).

For the validation, three variables were compared against IMOS data: sea surface elevation, zonal (u) and meridional (v) components of the current velocity. We performed a statistical analysis, including calculation of the skill score of the model with the Willmott's Skill Score (WSS):

$$WSS = 1 - \frac{\sum_{i=1}^{n}(O_i - S_i)^2}{\sum_{i=1}^{n}\left(|S_i - \overline{O}| + |O_i - \overline{O}|\right)^2},$$

where O_i are the observed values; S_i are the simulated values, $\overline{O}$ is the mean of the observations; and n is the number of observed/simulated values. A WSS of 1 indicates perfect model performance, while 0 means that the model doesn't bring more information than having a constant model using the mean value.

2.4. Dispersal model

Seagrass fragment dispersal was simulated with a Lagrangian Particle Tracker model (LPT) (Dimou and Adams, 1993; Spagnol et al., 2002). This particle tracker model uses the 2D hydrodynamic outputs to simulate dispersal of seagrass fragments. These "virtual" fragments were released every hour during 24 h periods, spaced by 5 days (i.e. 24 releases every 5 days). The total number of exported fragments per meadow was a function of its area (1 particle released per hour per km^2). The virtual propagules were released at random locations inside the meadow polygons. Release locations were sourced from a polygon map of seagrass developed by Carter et al. (2021). Individual polygons include information on seagrass species, including species presence, dominant species, density and surface area covered (Carter, McKenna, et al., 2021). The release locations were defined as polygons where a species group was dominant, meaning that the release locations depended on the species group considered.

The dispersal simulations were made for every month and every year, as fragments dispersal doesn't have a specific season. We did not focus on seagrass reproductive season as we model fragment dispersal rather than reproductive propagules (i.e. seeds, fruits, flowers). The simulation was stopped when all particles settled (i.e. reached their end of life) (Fig. 2). For example, during a January simulation, particles were released from 1st January to 31st January, with the simulation ending on the 28th of Feb for species of Group1, to allow all particles to disperse until the end of their buoyancy duration (defined in Table 1 and shown in Fig. 2). For this reason, only 6 years of dispersal were simulated, from 2011 to 2016, despite the 7-year hydrodynamic simulations (i.e. the December 2016 simulation ends in January/February 2017). A total of 432 simulations were run. This 6-year period allowed us to look at seasonal and interannual variations in fragment dispersal.

A biophysical behaviour was implemented for each species group based on three main stages of life post-fragmentation from the source meadow: positively buoyant, negatively buoyant, and no longer viable (Fig. 2). These life-history traits were applied to all species with species-dependent transition rates between states (Table 2). When a propagule is released from a meadow, it starts by being positively buoyant, which means that the propagule is floating at the sea surface and will be transported by both the ocean currents and a fraction (windage) of the wind velocity. After a certain duration (depending on the species and a random factor), it becomes negatively buoyant, meaning that the propagule goes down in the water column and is not influenced by the wind anymore but only by currents. Finally, when the propagule reaches the end of its buoyancy duration, we stop the transport of the propagule, and it is removed from the simulation. The transition between life-history states is governed by species-specific rates (see Table 2). The rates shown in Table 2 were established based on the literature and then refined by experts in seagrass ecology including co-authors of this study. The proportion of fragments in each state over the lifetime of each species is shown in Fig. 2.

We plotted data in order to visualise the sensitivity of windage on the dispersal distance of particles (Table 1). To do this, we used a random windage value, distributed within the range of values in Table 1, for every virtual propagule such that each single virtual propagule has its own windage, randomly chosen from the range provided in Table 1. For this sensitivity analysis, we sorted each particle from each species according to its windage value, by 0.1 % intervals, and then computed the dispersal distance associated with this windage value.

2.5. Statistical analysis

We implemented a Linear Mixed-effect Model (LMM) in Python using the package 'statsmodels' to investigate the physical and biological factors influencing long-distance seagrass dispersal in the Great Barrier Reef. In this analysis, we focused on dispersal distance without explicitly incorporating habitat presence or suitability at the settlement location because our primary objective was to quantify the physical and biological drivers that influence the potential for long-distance transport, providing a clearer understanding of the dispersal kernel that defines the spatial scale over which propagules can potentially move. Based on dispersal simulations, we calculated the dispersal distance by using the Euclidean distance between the release location and end of life location of each virtual propagule. This dispersal distance was used as the response variable in the LMM and was log-transformed to achieve normal distribution and heterogeneity of variances.

Explanatory variables used in the model were the result of an iteration process. We started with few variables, including windage and season (i.e. windy or not) and then improved the model by adding other variables. During this process we used the Akaike Information Criterion (AIC) to quantify model performance. AIC is a statistical metric calculating model performance by considering model complexity (i.e. too much complexity and too many variables will decrease model efficiency) and goodness of fit. The lower AIC value is the better the model is. In addition, we plotted the residuals to ensure that the model was representative (see Supp. materials Fig. S18). We ended up with this 4-variable model formula and repeated this model for each species group:

$$\log(\textbf{Dispersal distance}) = S + W + SOI + L + random(REI), \tag{4}$$

where S representing the seasonal cycle by capturing its cyclical variation. Since months are cyclical, we used a sine function to recognize patterns that repeat every twelve months. This approach allows the model to efficiently capture seasonality, as the onset and end of the season is variable. A higher value of S means a longer dispersal distance through the second half of the year (i.e. captured through the windy season). W represents the windage coefficient of the particle (as explained before); SOI is the Southern Oscillation Index (SOI) from the Bureau of Meteorology (BOM)[7] - quantifying the strength and phase of the El Nino-Southern Oscillation (ENSO). And L is the latitude of the initial position of the particle. An additional variable used in the analysis was the relative exposure index (REI) from (Grech, 2009) as random effect included in the LMM. This index is calculated using this formula:

$$REI = \sum_{i=1}^{16}(V_i \times P_i \times EF_i)\,, \tag{5}$$

where i is the ith compass heading (1 to 16 [N, NNE, NE, etc.]), in 22.5°

---

[7] http://www.bom.gov.au/climate/enso/soi/

increments; V is the average monthly wind speed (ms^{-1}), P is the percent (%) frequency of wind occurring in the ith direction, and EF is the effective fetch (m) (see (Grech, 2009) for more details). This exposure index estimates physical disturbance regimes within meadows. A high REI value for a meadow means that this meadow is exposed to stronger physical forces, while low REI value, i.e. a protected meadow will be more protected from the wind and therefore waves. Exposure values were calculated separately for the wet (November–April) and dry (May–October) seasons on a grid cell with 2 km resolution.

To present the dispersal variations through time and regions, we used the median dispersal distance due to the large differences in distance between all virtual particles. The median was therefore less sensitive to outliers compared to the mean distance. For each NRM region, we also calculated the Pearson correlation coefficients between species to assess temporal co-variation (cfr. Supp. materials Fig. S16).

3. Results

3.1. Ocean circulation model validation

Over the eight IMOS mooring stations, and the 7-year simulated for the ocean circulation, we calculated a mean Willmott's Skill Score of 0.89 for the sea elevation; 0.79 for u-component of the velocity and 0.66 for the v-component of the velocity (further details in supplementary materials – Tab. S1).

The SLIM model has the advantage to use an unstructured mesh, allowing finer resolution in areas of interest. We decided to set a 250 m resolution over seagrass meadows, as we wanted to reproduce as precisely as possible the seagrass dispersal dynamics at the meadow's scale. We calculated the averaged current speed and residual circulation over different seagrass meadows for four different locations (Fig. 3): Cairns and Green Island (Wet Tropics); Townsville and Magnetic Island (Burdekin); Whitsunday Islands (Mackay and Whitsunday) and Gladstone (Fitzroy). Residual circulation is variable over meadows and close to the coast, with eddies forming. Away from the coastal area, the residual circulation becomes more unidirectional. Having this fine resolution over meadows helps to capture small scale processes, such as eddies, that floating propagules could experience at their early stage of life or when settling down.

The GBR coastal circulation is complex, with numerous islands and bays, influencing currents direction and speed. Coastal current show different patterns thorough the GBR. In islands areas such as the Whitsundays, strong currents are observed, whereas in protected bays such as Cleveland Bay (Magnetic Island and Townsville) coastal currents are weaker (Fig. 3). Gladstone exhibits both of these characteristics, with sheltered bays formed by islands and added complexity from increased turbulence generated by numerous creeks entering from the land. Eddies in this area have much higher current speed compared to Cleveland Bay. Seagrass meadows are widespread over these multiple and diverse regions, mainly located in areas with weaker current magnitude. From a dispersal perspective, this resolution allows us to capture the large diversity of seagrass habitats (i.e. release locations) and their complex dispersal trajectories. Capturing the numerous eddies present will impact the local retention of dispersal outputs.

3.2. Windage sensitivity analysis

A higher windage value tends to increase fragment dispersal distance (Fig. 4). But this effect can be moderated by the season (windy or not windy). When winds are stronger (i.e. during windy season months), mainly during April-July, dispersal distance is at its peak. During this period, differences between the maximum and minimum windage could

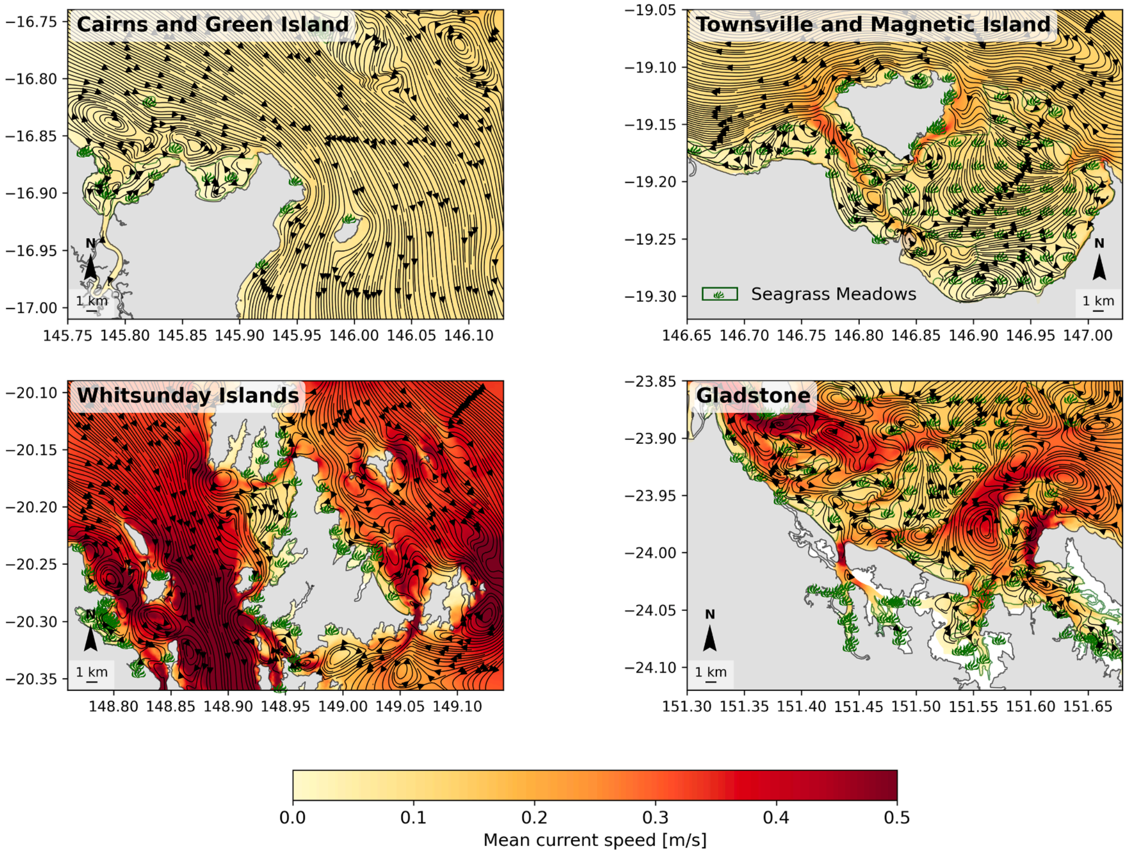

Fig. 3. Mean current speed (colormap) and residual circulation (stream plot) simulated for the month of March 2011. Four locations, where seagrass meadows are present (green plants), are shown to highlight current turbulence at meadow scale.

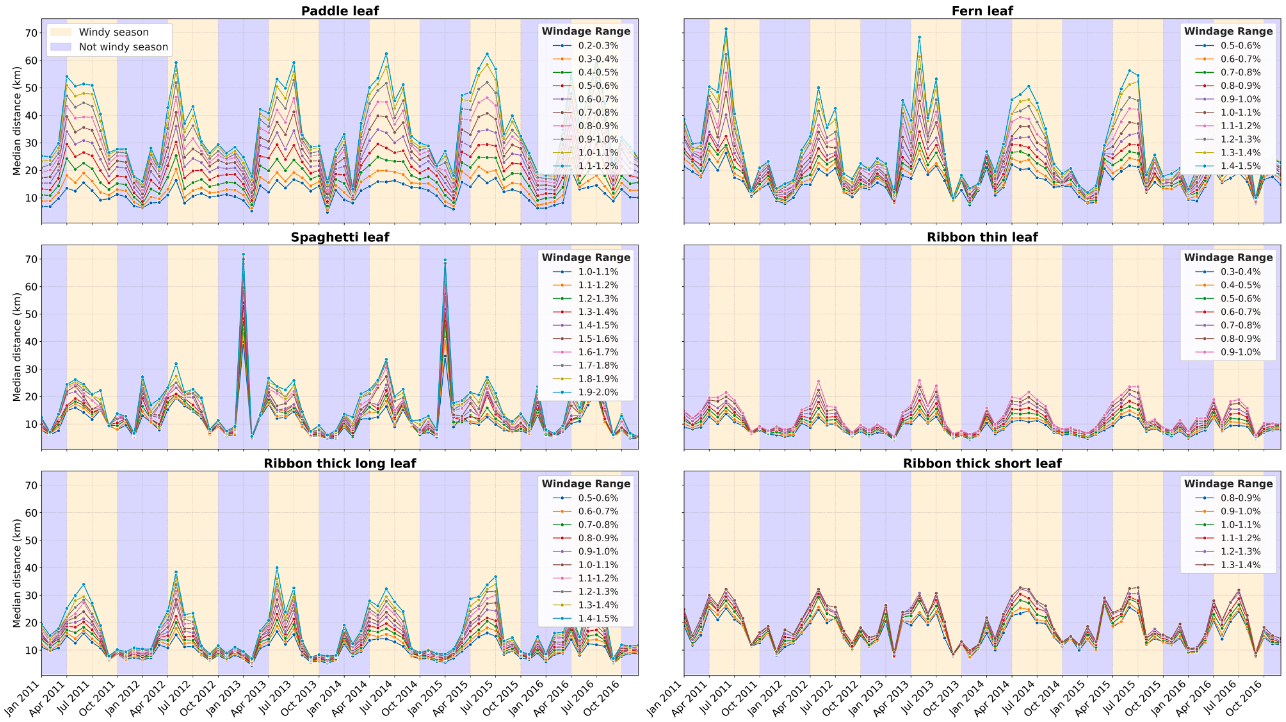

Fig. 4. Dispersal distance (kilometres) through time for seagrass fragments, classified by leaf morphology, in the entire GBR. Windage coefficients were classified by intervals of 0.1 %. The dispersal distance is expressed as the median of individual dispersal distance. Seasons are indicated with different colours – blue for the not windy season and orange for the windy season.

lead to a 40 km difference in dispersal distance (i.e. paddle leaf species in May 2012 and fern leaf species in May 2013). In other words, a change of 1 % in windage could lead to a 67 % increase in long distance dispersal (i.e. paddle leaf species May 2012).

During the not windy season, windage no longer influences dispersal distance, as weaker and more variable winds reduce its effect (Fig. 4). During this season, the median dispersal distance is almost the same with a maximum or a minimum windage value (i.e. ribbon thick short leaf species in September 2011, spaghetti and ribbon thick long leaf species in September 2016). This phenomenon is observed when dispersal distance is at its lowest, during the October-April period despite variations in between leaf morphologies.

Species are affected differently by windage due to variations in leaf morphology and life-history traits, particularly buoyancy duration. *Halophila* species (paddle and fern leaves species) show large variations between windages. Paddle leaf species have a relatively short total buoyancy duration (28 days across both positive and negative buoyancy phases; Fig. 2), limiting their capacity to disperse long distances except under maximum windage. By contrast, fern leaf species have the longest total buoyancy duration (70 days), but only a short period of positive buoyancy (i.e. ~7 days at the surface; Fig. 2). For paddle leaf species, however, positive buoyancy is longer (~14 days) relative to their shorter total buoyancy duration (28 days). Thus, we found that the proportion of time spent in the positively buoyant phase strongly influences the effect of windage on dispersal distance. Spaghetti leaf species (*S. isoetifolium*) has the largest windage among all species (2 %) and is also the least common species in its distribution (5 meadows). This species is therefore very sensitive to windage, with these two peaks observed in January 2013 and January 2015. Windage has less impact on the three other groups (ribbon leaf species) compared to paddle and fern leaf species. These species have a similar leaf shape (ribbon) and a same maximum buoyancy duration (56 days). They observed a 10 km difference in dispersal distance between the lowest and highest windage values, with a maximum distance of 20 km for ribbon thick long leaf. But the ribbon thin and ribbon thick short leaf species have a smaller windage range (0.7 % variation and 0.6 % respectively), leading to smaller differences between Min and Max windages.

3.3. Dispersal variations by species group and through space and time

Our model results revealed strong seasonal variations in dispersal distances for the six seagrass groups (Fig. 5), influenced by the two seasons (windy and not windy) and their associated wind conditions. Long distance dispersal events mostly occur during the January-July period (long dispersal starts at the end of wet season but peak during dry season). Amplitudes of these seasonal variations differ between species and regions, but variations in dispersal distance can also be large within the same season, region and species. As an example, for paddle leaf propagules of Cape York, the minimum dispersal distance over not windy seasons was 0.02 km while the maximum recorded for the same season reached 350 km (cfr. Supp. materials Tab. S2).

The six NRM regions used to segment the analysis in similar biogeographic regions show different seagrass dispersal dynamics in terms of amplitude and seasonality (Fig. 5). In the Wet Tropics, Burdekin, Mackay & Whitsunday, and Fitzroy, all seagrass species groups have a higher median travelled distance during the windy season than during the not windy season (cfr. Supp. materials Tab. S2), which aligns with the intensity of the Trade Winds. In Cape York and Burnett-Mary, the trend is less clear, with some species having a higher dispersal distance during the not windy season (i.e. all ribbon leaf species in Cape York and fern leaf species in Burnett-Mary). Each NRM region has its own seasonal pattern, with sometimes large differences in amplitude. As an example, paddle leaf species exhibit a large increase in dispersal distance during the windy season compared to the not windy season in Cape York (30.46 km in average distance, 17.6 km in median distance). However, in the Wet Tropics, these same species have a reduced seasonality (increase during windy season of 7.02 km in average; increase of 5.11 km for median).

Different seagrass species exhibit different dispersal patterns (Fig. 5). Spaghetti (*S. isoetifolium* – high windage) and fern (*H. spinulosa* – long

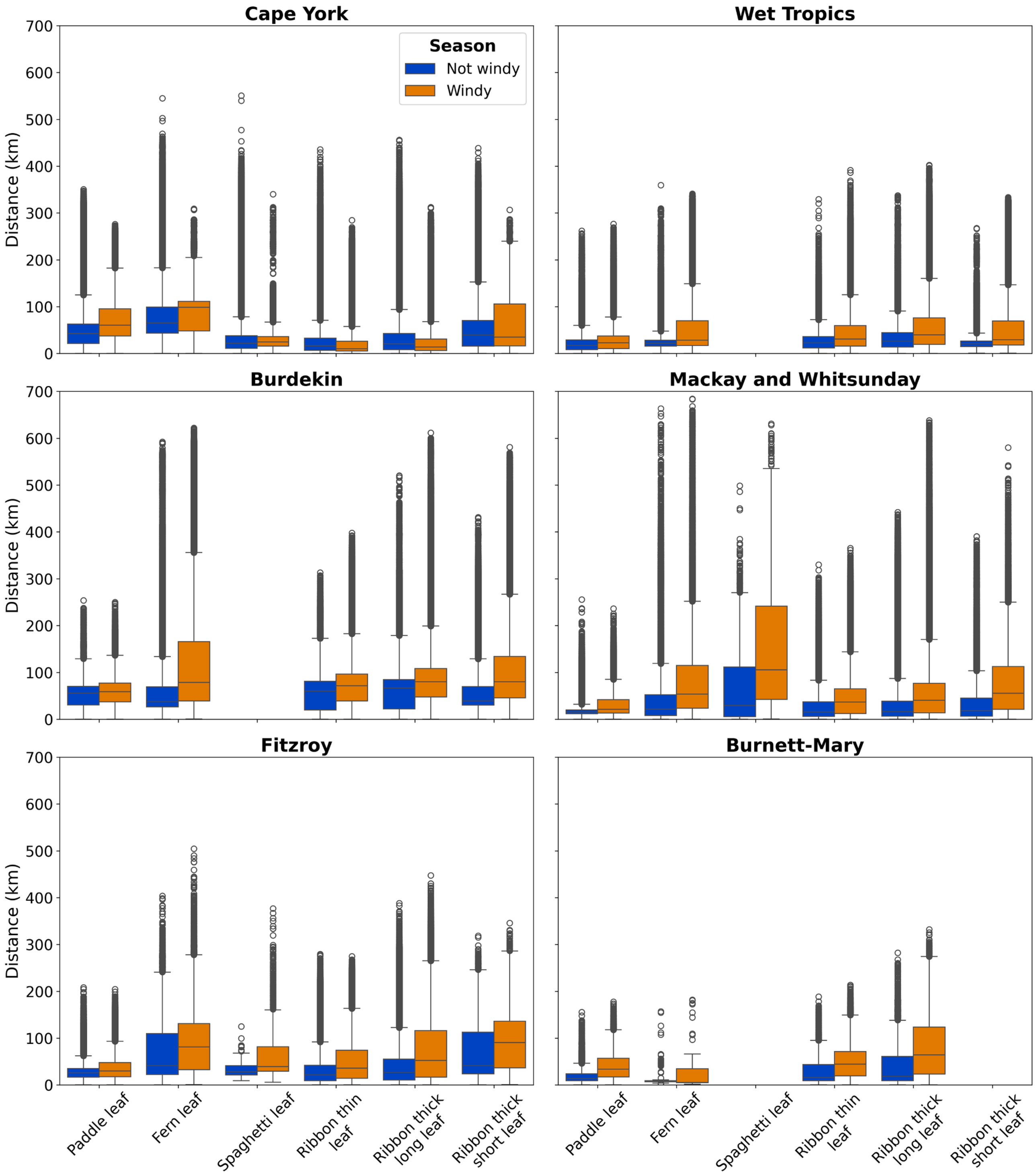

Fig. 5. boxplots of the dispersal distances (kilometres) in each NRM region and for all species groups. These distances were computed for the 6-year period, differentiating two seasons according to wind pattern: not windy season (October-March, in blue) and windy season (April-September, in orange).

buoyancy duration) leaf species are more likely to travel long distances, with maximum recorded distances of 631 km and 684 km respectively. Despite this common characteristic these two species are only weakly to moderately correlated in their dispersal patterns (0.22 in Cape York; 0.88 in Mackay and Whitsunday; and 0.45 in Fitzroy – Supp. materials Fig. S16). The most correlated species in their dispersal patterns were ribbon thin and ribbon thick long leaf species with correlations ranging from 0.93 in Cape York to 0.98 in Wet Tropics, Mackay & Whitsunday and Fitzroy. This makes sense as these two groups represent the same species (except *C. rotundata*), meaning same release locations, with different morphologies (and therefore windage). Paddle leaf species have the shortest buoyancy duration of the model (28 days) and is the species group that disperses the less, except for Cape York region, where this species is more abundant (73 meadows over the 304). These species are correlated with ribbon thick long leaf species in few regions (0.94 in Wet Tropics; 0.87 in Fitzroy and 0.89 in Burnett-Mary). This is interesting considering their very different leaf sizes, which suggests the correlation may be driven by their co-occurrence within dominant meadows in the spatial layer.

3.4. *Factors influencing dispersal (LMM)*

Outputs of the LMMs to assess the influence of different variables on dispersal distance are provided in the supplementary materials – (Fig. S17). All variables tested in the model were significant ($p < 0.05$). Among the variables tested, the relative exposure index exhibited the strongest effect on long-distance dispersal. In the context of the LMM, this means that for each unit increase in REI, the predicted dispersal distance increases by an amount corresponding to the coefficient — ranging from 0.45 for paddle leaf species to 25.88 for the spaghetti leaf species (*Syringodium isoetifolium*). This exposure index plays an important role for this last group, which can partly explain the two peaks in dispersal in Fig. 4. As this species is the least common and has the largest windage value, a highest exposure correlated with stronger winds can lead to very long dispersal (up to 631.11 km). Seasonal variations, and windage come with the second highest coefficients. Windage is more important for paddle and ribbon thin leaf species, while the other species groups express stronger seasonal variations. Latitudinal gradient is an important variable, but its effect is moderate on distance travelled. Except for paddle leaf species, all propagules tend to have a higher dispersal distance the more southern their source location. The last variable in the model was the SOI. While the SOI was statistically significant ($p < 0.05$), its coefficient was relatively small, indicating a limited influence on dispersal distance. This suggests that although ENSO-related variability had a detectable effect within the model, its overall impact was not evident over the six-year period. One possible explanation is that the considered was too short to fully capture the influence of larger-scale climate oscillations such as El Niño, despite the presence of a strong event in 2015. This coefficient is slightly positive for fern leaf, ribbon thin, ribbon thick long and ribbon thick short species (0.005, 0.001, 0.001, 0.002 respectively), while negative for all other species (−0.001 and −0.002 for paddle and spaghetti leaf species – see supplementary materials).

4. Discussion

We combined high-resolution biophysical modelling with species-specific biological data to evaluate the long-distance dispersal potential of coastal seagrass meadows in the GBR. Using the SLIM model, we simulated ocean circulation across a 7-year period to capture the hydrodynamic processes shaping seagrass dispersal across coastal ecosystems. A species-specific particle tracking model was then implemented to predict the dispersal of fragments, incorporating life-history traits of 11 GBR seagrass species grouped into six morphological classes. Our findings provide new insights into: (1) the influence of windage variability on long-distance dispersal; (2) the spatial and temporal dispersal dynamics of seagrass fragments, shaped by species' life-history traits; and (3) the relative contribution of biophysical drivers to dispersal distance. By integrating biological traits with physical transport processes, this study advances understanding of the mechanisms that underpin seagrass recovery and resilience in the GBR (Unsworth et al., 2015), while also identifying key knowledge gaps in seagrass movement ecology. The species-specific particle tracking approach applied here represents a critical step towards capturing both biological and biophysical complexities of seagrass dispersal and highlights the need for greater species-level resolution in biophysical dispersal models.

We found that seasonal variation strongly influences long distance dispersal of seagrass fragments in the GBR, with high dispersal distances occurring during the windy season. This contrasts with the main sexual reproductive period of seagrasses, which occurs primarily at the end of the dry season/beginning of the wet season, when dispersal distance is decreasing (September to November, (Collier et al., 2021)). Since sexual reproduction relies largely on the dispersal of seeds and/or fruits (Ackerman, 2006), these results suggest that sexually produced propagules are more likely to disperse over shorter distances during the reproductive period, compared to vegetative fragments (see Fig. 5). In contrast, long distance dispersal events are more likely to occur during the windy season via vegetative fragments, although some exceptions were found (i.e. in Cape York and Burnett-Mary - Fig. 5). Overall, this indicates that sexual reproduction mostly occurring during the not windy season likely plays a greater role in maintaining local resilience through short-distance dispersal and recruitment into neighbouring meadows, while vegetative fragment dispersal during the windy season contributes more to broader spatial dispersal and connectivity.

The GBR's coastal topography plays a crucial role in shaping seagrass dispersal patterns, leading to significant regional variability. We assessed this role using both the relative exposure index and initial latitude in the LMM, while also segmenting the domain according to NRM regions. The results revealed that seagrass meadows with higher relative exposure index – located along less sheltered coastlines – tended to generate fragments that dispersed over longer distances. This pattern is even more pronounced in the southern GBR, where NRM regions such as Mackay & Whitsunday and Fitzroy show higher exposure levels, likely due to limited coastal shielding and broader continental shelf width. In contrast, northern regions like Cape York exhibit lower exposure, with more sheltered coastlines, leading to smaller dispersal. These findings support the idea that regional hydrodynamic and biogeographic conditions, as captured by both the exposure index and NRM segmentation, are key drivers of seagrass dispersal in the GBR (Grech, 2009).

We found that both species leaf morphology (i.e. windage), and buoyancy duration influence seagrass long distance dispersal potential. The combination of high windage and long buoyancy duration (i.e. fern leaf species – *H. spinulosa*) or long surface buoyancy duration (i.e. spaghetti leaf species – *S. isoetifolium*) leads to a higher long distance dispersal potential. In contrast, small buoyancy duration and small windage is linked to a smaller dispersal potential (cfr. Paddle leaf seagrasses). However, this is not always the case as we also found a high correlation in dispersal distance between paddle leaf and ribbon thick long leaf seagrasses, which vary in leaf morphology and buoyancy duration, suggesting an additional complexity. Meadow distribution might explain this correlation, as these species (i.e. *H. ovalis, Z. muelleri, H. uninervis*) are found in similar habitats, such as estuaries, which isolate them from wind and waves exposure in the GBR (Carter, Collier, et al., 2021). These genera (i.e. *Halophila, Zostera* and *Halodule*) are recognized as colonizing species, indicating similarities in their dispersal strategies (Kilminster et al., 2015). As colonizing species, they can quickly exploit and colonize new areas, stabilize sediments and improve water quality providing the conditions for more persistent species to colonize as part of ecological succession. In our study, these species, particularly *H. spinulosa* (fern leaves), exhibited among the greatest dispersal potentials. This demonstrates their capacity to colonize new areas over broad spatial scales and highlights their importance for seagrass conservation strategies.

Windage has a clear effect on seagrass long distance dispersal, as highlighted by both the statistical analysis and the sensitivity analysis. By incorporating data from flume tank studies (Lai et al., 2020; Tol et al., 2024) and expert knowledge, we used refined and smaller windage values, compared to previous modelling research (see Table 1). As a result, we obtained different predicted dispersal distances. Our maximum predicted dispersal distance was 684 km (fern leaf species) while Grech et al. (2016), with a constant windage of 2 %, had a maximum distance of 950 km. Dispersal distance does not only reflect windage, but our maximum dispersal distance was using a larger maximum buoyancy duration (fern leaf species, 70 days) than the one used in Grech et al. (2016) (i.e. 56 days). This means that for a longer dispersal time, we have a lower dispersal distance, suggesting the importance of the windage and propagules buoyancy duration. In addition, our sensitivity analysis revealed that windage can indeed increase the dispersal distance but windage is also region and season dependant (see Fig. 5). An increase by 1 % in windage is large and can lead to an increase of 40 km in dispersal distance. Our results demonstrate that the value of windage is crucial when defining biological parameters in biophysical models of dispersal.

From a management perspective, our study highlights the variability in seagrass long distance dispersal in the GBR. Conservation planning that relies on natural recovery mechanisms (i.e. fragment dispersal), should consider species-specific traits of the targeted species, including their buoyancy duration and windage, to inform management strategies. Regional variation is also critical, as different locations will be exposed to distinct biological and physical conditions, including varying wind and waves exposure. Integrating this level of specificity into decision-making processes can improve the effectiveness of coastal management strategies, particularly for guiding the scaling of restoration activities, the design of protected areas and the management of coastal developments such as ports and urban settlements.

As with any modelling study, it is important to understand the assumptions underlying the model. For the hydrodynamic simulations, we used the 2D version of the SLIM model, assuming that the coastal region of the GBR is vertically well-mixed (Grech et al., 2016; Luick et al., 2007). This hypothesis is supported by the shallow nature of the studied area, with a mean depth of 35 m on the shelf (Wolanski et al., 2024) (Fig. 1A), and by extensive field and modelling evidence showing predominantly barotropic flow with limited, localized vertical variability (Saint-Amand, 2022; Thomas et al., 2015). Therefore, a 2D model can capture the essential horizontal transport dynamics while enabling higher spatial resolution than a 3D model. Wetting and drying processes were not considered in the current model. This choice was motivated by the large spatial extent of the domain and the need to ensure numerical stability. Although some shallow coastal features such as seagrass meadows may experience partial exposure during low tides, our model focused on long distance dispersal occurring over large spatial (> 100 km) and temporal (several weeks) scales. Over those scales, the importance of the wetting-drying dynamics is secondary. However, their inclusion could be an additional complexity for future modelling studies, particularly if the focus is on local dispersal patterns and settlement processes where seagrass propagules could settle on dry areas.

The seagrass distribution layer used in the dispersal model is fixed throughout the simulated period and is based on the maximum recorded distributions of historical data. However, it does not represent the real seagrass distribution that was observed during the study period. As this was the only data available, we used this dataset but more nuanced temporally resolved seagrass data would provide more accurate dispersal estimates. Additionally, we only considered release locations where the species were classified as “dominant” in the different meadows. The reason behind this choice is that, given the variability of seagrass cover in the GBR, focusing on core habitats with optimal growth conditions increases the likelihood that these areas act as major sources of propagules. However, reality is that some species could have generated fragments across a much more expanded spatial area as they are present as smaller proportion in other meadows (as example *S. isoetifolium* who is a common species in the GBR (Carter, Collier, et al., 2021)). This study should be used as a reference to compare our dispersal estimates, likely to be underestimated, with future estimates of the full potential of seagrass dispersal in the GBR.

Our biological parameters assumed that leaf morphology was the primary driver for windage, and our species classification was based on that. Given the lack of species-specific empirical windage coefficients for all species, using leaf morphology as a proxy allowed us to apply a consistent and ecologically meaningful classification framework. Regarding the assumptions made for the different life stages of the fragments, they were established with the literature available and then visually refined, through guesstimate plots, by seagrass experts including co-authors of this paper. These life-stages should be refined when more empirical data will be available. Seagrass fragments are very variable, even within a same species they are likely to be considerably different in their traits (size, number of shoots per fragments, rhizome length - (Lin et al., 2024)). This model standardizes seagrass fragments, further development could aim to do single-species dispersal models with specific-species data (that are not available now for all species).

Future dispersal modelling research should aim to consider a longer time period, particularly to assess the influence of large-scale climate variability, such as ENSO. Despite a strong El Nino year in 2015, our research suggests that ENSO effects were not evident over the six-year period selected. Longer simulations (10 years), including both strong El Niño and La Niña phases, could provide new insights into how extreme climatic events impact seagrass dispersal and persistence. In addition to ENSO, cyclones, that are predicted to be less numerous but of higher intensity in the GBR (Lavender and Walsh, 2011), would be another factor to consider in future research. Indeed, tropical cyclones are associated with strong winds and waves, but also freshwater and sediment that will alter seagrass dispersal (Connolly et al., 2018; Correia and Smee, 2022). In addition to these climatic drivers and changes, assessing dispersal with a temporally resolved distribution layer that match the studied period would further improve the accuracy of predictions, enhance ecosystem-based management approaches, and support the long-term conservation of seagrass meadows in the GBR and beyond. Here we provided a first attempt of a large-scale dispersal biophysical model for seagrass long distance dispersal. This integrates a complex biological behaviour, considering 11 seagrass species, over a 6-year period.

5. Conclusion

This study presents a framework to incorporate the diversity of seagrass species-specific traits and variability of bioregional conditions in dispersal biophysical models. Through the use of refined parameters, often missing in observational studies, along with high-resolution modelling and segmentation based on coastal topography, we highlighted key drivers of marine coastal dispersal. For tropical seagrasses, this approach revealed substantial variability in dispersal patterns, significantly influencing model outcomes. As climate change alters ocean circulation and the environmental drivers shaping marine dispersal, advancing dispersal biophysical models is crucial to reflect these changes and support effective management strategies. Although developed in the context of the Great Barrier Reef, this approach can be adapted to other coastal ecosystems facing similar challenges.

CRediT authorship contribution statement

Douchan Hanuise: Writing – review & editing, Writing – original draft, Visualization, Software, Resources, Project administration, Methodology, Investigation, Formal analysis, Data curation, Conceptualization. **Thomas Dobbelaere:** Writing – review & editing, Supervision, Software, Data curation. **Severine Choukroun:** Writing – review & editing, Validation, Supervision, Software. **Michael A. Rasheed:** Writing – review & editing, Validation, Supervision. **Jonathan Lambrechts:** Supervision, Software. **Paul H. York:** Writing – review & editing, Validation, Conceptualization. **Timothy M. Smith:** Writing – review & editing, Validation, Conceptualization. **Robert G. Coles:** Writing – review & editing. **Emmanuel Hanert:** Writing – review & editing, Validation, Supervision, Methodology. **Alana Grech:** Writing – review & editing, Validation, Supervision, Methodology, Conceptualization.

Declaration of competing interest

The authors declare that they have no known competing financial interests or personal relationships that could have appeared to influence the work reported in this paper.

Acknowledgements

Funding for this research was provided by James Cook University and the Australian Research Council (LP210300851). Computational resources have been provided by the supercomputing facilities of the Université catholique de Louvain (CISM/ UCLouvain); the Consortium des Équipements de Calcul Intensif en Fédération Wallonie Bruxelles (CECI) funded by the Fonds de la Recherche Scientifique de Belgique (F. R.S.-FNRS) under convention 2.5020.11 and by MeluXina HPC funded jointly by the EuroHPC Joint Undertaking, through the European Union's Connecting Europe Facility and the Horizon 2020 research and innovation programme, as well as the Grand Duché du Luxembourg. We extend our sincere gratitude to all the participants in the expert knowledge meeting for generously sharing their invaluable expertise on tropical seagrasses.

Supplementary materials

Supplementary material associated with this article can be found, in the online version, at doi:10.1016/j.ecolmodel.2025.111329.

Data availability

Data will be made available on request.

References

Ackerman, J.D., 2006. Sexual reproduction of seagrasses: pollination in the marine context. In: Larkum, A.W.D., Orth, R.J., Duarte, C.M. (Eds.), Seagrasses: Biology, Ecology and Conservation. Springer, Netherlands, pp. 89–109. https://doi.org/10.1007/978-1-4020-2983-7_4.

Álvarez-Noriega, M., Burgess, S.C., Byers, J.E., Pringle, J.M., Wares, J.P., Marshall, D.J., 2020. Global biogeography of marine dispersal potential. Nat. Ecol. Evol. (N Y) 4 (9), 1196–1203. https://doi.org/10.1038/s41559-020-1238-y.

Beaman, R.J., 2017. High-resolution depth model for the Great Barrier Reef - 30 m. Geosci. Aust. https://doi.org/10.4225/25/5a207b36022d2.

Brodie, G., Holland, E., N'Yeurt, A.D.R., Soapi, K., Hills, J., 2020. Seagrasses and seagrass habitats in Pacific small island developing states: potential loss of benefits via human disturbance and climate change. Mar. Pollut. Bull. 160, 111573. https://doi.org/10.1016/j.marpolbul.2020.111573.

Brodie, J., Waterhouse, J., 2012. A critical review of environmental management of the 'not so great' Barrier Reef. Estuar. Coast. Shelf. Sci. 104-105, 1–22. https://doi.org/10.1016/j.ecss.2012.03.012.

Brown, J.H., 2014. Why marine islands are farther apart in the tropics. Am. Nat. 183 (6), 842–846. https://doi.org/10.1086/676015.

Cai, W., Santoso, A., Collins, M., Dewitte, B., Karamperidou, C., Kug, J.-S., Lengaigne, M., McPhaden, M.J., Stuecker, M.F., Taschetto, A.S., Timmermann, A., Wu, L., Yeh, S.-W., Wang, G., Ng, B., Jia, F., Yang, Y., Ying, J., Zheng, X.-T., Zhong, W., 2021. Changing El Niño–Southern oscillation in a warming climate. Nat. Rev. Earth Environ. 2 (9), 628–644. https://doi.org/10.1038/s43017-021-00199-z.

Carter, A.B., Collier, C., Lawrence, E., Rasheed, M.A., Robson, B.J., Coles, R., 2021a. A spatial analysis of seagrass habitat and community diversity in the Great Barrier Reef World Heritage Area. Sci. Rep. 11 (1), 22344. https://doi.org/10.1038/s41598-021-01471-4.

Carter, A.B., McKenna, S.A., Rasheed, M.A., Collier, C., McKenzie, L., Pitcher, R., Coles, R., 2021b. Synthesizing 35 years of seagrass spatial data from the Great Barrier Reef World Heritage Area, Queensland, Australia. Limnol. Oceanogr. Lett. 6 (4), 216–226. https://doi.org/10.1002/lol2.10193.

Chand, S.S., Tory, K.J., Ye, H., Walsh, K.J.E., 2017. Projected increase in El Niño-driven tropical cyclone frequency in the Pacific. Nat. Clim. Chang. 7 (2), 123–127. https://doi.org/10.1038/nclimate3181.

Choukroun, S., Ridd, P.V., Brinkman, R., McKinna, L.I.W., 2010. On the surface circulation in the western Coral Sea and residence times in the Great Barrier Reef. J. Geophys. Res.: Oceans 115 (C6). https://doi.org/10.1029/2009JC005761.

Coles, R.G., Rasheed, M.A., McKenzie, L.J., Grech, A., York, P.H., Sheaves, M., McKenna, S., Bryant, C., 2015. The Great Barrier Reef World Heritage Area seagrasses: managing this iconic Australian ecosystem resource for the future. Estuar. Coast. Shelf. Sci. 153, A1–A12. https://doi.org/10.1016/j.ecss.2014.07.020.

Collier, C.J., Carter, A.B., Rasheed, M., McKenzie, L., Udy, J., Coles, R., Brodie, J., Waycott, M., O'Brien, K.R., Saunders, M., Adams, M., Martin, K., Honchin, C., Petus, C., Lawrence, E., 2020. An evidence-based approach for setting desired state in a complex Great Barrier Reef seagrass ecosystem: a case study from Cleveland Bay. Environ. Sustain. Indic. 7, 100042. https://doi.org/10.1016/j.indic.2020.100042.

Collier, C.J., Langlois, L., Waycott, M., McKenzie, L.J., 2021. *Resilience in practice: development of a seagrass resilience metric for the Great Barrier Reef Marine Monitoring Program* (Marine Monitoring Program. Issue. G. B. R. M. P. Auth. https://hdl.handle.net/11017/3904.

Connolly, R.M., Jackson, E.L., Macreadie, P.I., Maxwell, P.S., O'Brien, K.R, 2018. Seagrass dynamics and resilience. In: Larkum, A.W.D., Kendrick, G.A., Ralph, P.J. (Eds.), Seagrasses of Australia: Structure, Ecology and Conservation. Springer International Publishing, pp. 197–212. https://doi.org/10.1007/978-3-319-71354-0_7.

Correia, K.M., Smee, D.L., 2022. A meta-analysis of Tropical Cyclone effects on Seagrass Meadows. Wetlands 42 (8), 108. https://doi.org/10.1007/s13157-022-01611-0.

Corte, G.N., Gonçalves-Souza, T., Checon, H.H., Siegle, E., Coleman, R.A., Amaral, A.C.Z, 2018. When time affects space: dispersal ability and extreme weather events determine metacommunity organization in marine sediments. Mar. Environ. Res. 136, 139–152. https://doi.org/10.1016/j.marenvres.2018.02.009.

Cowen, R.K., Sponaugle, S., 2009. Larval dispersal and marine population connectivity. Ann. Rev. Mar. Sci. 1, 443–466. https://doi.org/10.1146/annurev.marine.010908.163757, 12009.

Critchell, K., Grech, A., Schlaefer, J., Andutta, F.P., Lambrechts, J., Wolanski, E., Hamann, M., 2015. Modelling the fate of marine debris along a complex shoreline: lessons from the Great Barrier Reef. Estuar. Coast. Shelf. Sci. 167, 414–426. https://doi.org/10.1016/j.ecss.2015.10.018.

Day, J.C., Dobbs, K., 2013. Effective governance of a large and complex cross-jurisdictional marine protected area: australia's Great Barrier Reef. Mar. Policy. 41, 14–24. https://doi.org/10.1016/j.marpol.2012.12.020.

de los Santos, C.B., Olivé, I., Moreira, M., Silva, A., Freitas, C., Araújo Luna, R., Quental-Ferreira, H., Martins, M., Costa, M.M., Silva, J., Cunha, M.E., Soares, F., Pousão-Ferreira, P., Santos, R., 2020. Seagrass meadows improve inflowing water quality in aquaculture ponds. Aquaculture 528, 735502. https://doi.org/10.1016/j.aquaculture.2020.735502.

De los Santos, C.B., Scott, A., Arias-Ortiz, A., Jones, B., Kennedy, H., Mazarrasa, I., McKenzie, L., Nordlund, L.M., de la Torre-Castro, M.d.l.T., Unsworth, R.K.F., Ambo-Rappe, R., 2020. *Seagrass ecosystem services: assessment and scale of benefits*. U. N. Environment. http://hdl.handle.net/10400.1/14722.

Dimou, K.N., Adams, E.E., 1993. A random-walk, particle tracking model for well-mixed estuaries and coastal waters. Estuar. Coast. Shelf. Sci. 37 (1), 99–110. https://doi.org/10.1006/ecss.1993.1044.

Dobbelaere, T., Dekens, A., Saint-Amand, A., Alaerts, L., Holstein, D.M., Hanert, E., 2024. Hurricanes enhance coral connectivity but also superspread coral diseases. Glob. Chang. Biol. 30 (6), e17382. https://doi.org/10.1111/gcb.17382.

Duarte, C.M., 1991. Allometric scaling of seagrass form and productivity. Mar. Ecol. Prog. Ser 77, 289–300. https://www.int-res.com/articles/meps/77/m077p289.pdf.

Egbert, G.D., Erofeeva, S.Y., 2002. Efficient inverse modeling of barotropic ocean tides. J. Atmos. Ocean. Technol. (Singap World Sci) 19 (2), 183–204. https://doi.org/10.1175/1520-0426(2002)019<0183:EIMOBO>2.0.CO;2.

Evans, R.D., McMahon, K.M., van Dijk, K.J., Dawkins, K., Nilsson Jacobi, M., Vikrant, A., 2021. Identification of dispersal barriers for a colonising seagrass using seascape genetic analysis. Sci. Total Environ. 763, 143052. https://doi.org/10.1016/j.scitotenv.2020.143052.

Figueiredo, J., Thomas, C.J., Deleersnijder, E., Lambrechts, J., Baird, A.H., Connolly, S. R., Hanert, E., 2022. Global warming decreases connectivity among coral populations. Nat. Clim. Chang. 12 (1), 83–87. https://doi.org/10.1038/s41558-021-01248-7.

Grech, A., 2009. Spatial Models and Risk Assessments to Inform Marine Planning At ecosystem-scales: Seagrasses and Dugongs As a Case Study. James Cook University]. PhD thesis.

Grech, A., Chartrand-Miller, K., Erftemeijer, P., Fonseca, M., McKenzie, L., Rasheed, M., Taylor, H., Coles, R., 2012. A comparison of threats, vulnerabilities and management approaches in global seagrass bioregions. Environ. Res. Lett. 7 (2), 024006. https://doi.org/10.1088/1748-9326/7/2/024006.

Grech, A., Hanert, E., McKenzie, L., Rasheed, M., Thomas, C., Tol, S., Wang, M., Waycott, M., Wolter, J., Coles, R., 2018. Predicting the cumulative effect of multiple disturbances on seagrass connectivity. Glob. Chang. Biol. 24 (7), 3093–3104. https://doi.org/10.1111/gcb.14127.

Grech, A., Wolter, J., Coles, R., McKenzie, L., Rasheed, M., Thomas, C., Waycott, M., Hanert, E., 2016. Spatial patterns of seagrass dispersal and settlement. Divers. (Basel) Distrib. 22 (11), 1150–1162. https://doi.org/10.1111/ddi.12479.

Gurdek-Bas, R., Benthuysen, J.A., Harrison, H.B., Zenger, K.R., van Herwerden, L., 2022. The El Niño Southern Oscillation drives multidirectional inter-reef larval connectivity in the Great Barrier Reef. Sci. Rep. 12 (1), 21290. https://doi.org/10.1038/s41598-022-25629-w.

Huang, Z., Feng, M., Dalton, S.J., Carroll, A.G., 2024. Marine heatwaves in the Great Barrier Reef and Coral Sea: their mechanisms and impacts on shallow and mesophotic coral ecosystems. Sci. Total Environ. 908, 168063. https://doi.org/10.1016/j.scitotenv.2023.168063.

Jackson, E.L., Smith, T.M., York, P.H., Nielsen, J., Irving, A.D., Sherman, C.D.H., 2021. An assessment of the seascape genetic structure and hydrodynamic connectivity for subtropical seagrass restoration. Restor. Ecol. 29 (1), e13269. https://doi.org/10.1111/rec.13269.

Jahnke, M., Jonsson, P.R., 2022. Biophysical models of dispersal contribute to seascape genetic analyses. Philos. Trans. R. Soc. B: Biol. Sci. 377 (1846), 20210024. https://doi.org/10.1098/rstb.2021.0024.

Jahnke, M., Moksnes, P.-O., Olsen, J.L., Serra Serra, N., Nilsson Jacobi, M., Kuusemäe, K., Corell, H., Jonsson, P.R., 2020. Integrating genetics, biophysical, and demographic insights identifies critical sites for seagrass conservation. Ecol. Appl. 30 (6), e02121. https://doi.org/10.1002/eap.2121.

Kendrick, G.A., Orth, R.J., Statton, J., Hovey, R., Ruiz Montoya, L., Lowe, R.J., Krauss, S. L., Sinclair, E.A., 2017. Demographic and genetic connectivity: the role and consequences of reproduction, dispersal and recruitment in seagrasses. Biol. Rev. Camb. Philos. Soc. 92 (2), 921–938. https://doi.org/10.1111/brv.12261.

Kilminster, K., McMahon, K., Waycott, M., Kendrick, G.A., Scanes, P., McKenzie, L., O'Brien, K.R., Lyons, M., Ferguson, A., Maxwell, P., Glasby, T., Udy, J., 2015. Unravelling complexity in seagrass systems for management: australia as a microcosm. Sci. Total Environ. 534, 97–109. https://doi.org/10.1016/j.scitotenv.2015.04.061.

Kuusemäe, K., von Thenen, M., Lange, T., Rasmussen, E.K., Pothoff, M., Sousa, A.I., Flindt, M.R., 2018. Agent based modelling (ABM) of eelgrass (Zostera marina) seedbank dynamics in a shallow Danish estuary. Ecol. Modell. 371, 60–75. https://doi.org/10.1016/j.ecolmodel.2018.01.001.

Lai, S., Cheok, Z.Y., Bouma, T.J., Yaakub, S.M., Todd, P.A., 2020. The relative importance of light and hydrodynamics in the decay and transport of vegetative seagrass fragments. Estuar. Coast. Shelf. Sci. 232, 106430. https://doi.org/10.1016/j.ecss.2019.106430.

Lai, S., Teo, T.Z.E., Rullyanto, A., Low, J., Tun, K., Todd, P.A., Yaakub, S.M., 2024. An agent-based model approach to assessing the role of vegetative fragments in seagrass connectivity [Article]. Ecol. Modell. 487, 110528. https://doi.org/10.1016/j.ecolmodel.2023.110528. Article.

Lambrechts, J., Hanert, E., Deleersnijder, E., Bernard, P.-E., Legat, V., Remacle, J.-F., Wolanski, E., 2008. A multi-scale model of the hydrodynamics of the whole Great Barrier Reef. Estuar. Coast. Shelf. Sci. 79 (1), 143–151. https://doi.org/10.1016/j.ecss.2008.03.016.

Lavender, S.L., Walsh, K.J.E., 2011. Dynamically downscaled simulations of Australian region tropical cyclones in current and future climates. Geophys. Res. Lett. 38 (10). https://doi.org/10.1029/2011GL047499.

Lett, C., Ayata, S.-D., Huret, M., Irisson, J.-O., 2010. Biophysical modelling to investigate the effects of climate change on marine population dispersal and connectivity. Prog. Ocean. 87 (1), 106–113. https://doi.org/10.1016/j.pocean.2010.09.005.

Lin, C., Coles, R.G., Rasheed, M.A., Grech, A., 2024. A comprehensive functional trait database of seagrasses in tropical Queensland. Aust. J. Bot 72 (8). https://doi.org/10.1071/BT24017.

Luick, J.L., Mason, L., Hardy, T., Furnas, M.J., 2007. Circulation in the Great Barrier Reef Lagoon using numerical tracers and in situ data. Cont. Shelf. Res. 27 (6), 757–778. https://doi.org/10.1016/j.csr.2006.11.020.

McKenzie, L.J., Collier, C.J., Langlois, L.A., Yoshida, R.L., 2023. Mar. Monit. Program Annu. Rep. 2021-22 Inshore Seagrass Monit. https://hdl.handle.net/11017/3999.

McKenzie, L.J., Langlois, L.A., Roelfsema, C.M., 2022. Improving approaches to mapping seagrass within the Great Barrier Reef: from field to spaceborne earth observation. Remote Sens. (Basel) 14 (11), 2604. https://www.mdpi.com/2072-4292/14/11/2604.

McMahon, K., van Dijk, K.-j., Ruiz-Montoya, L., Kendrick, G.A., Krauss, S.L., Waycott, M., Verduin, J., Lowe, R., Statton, J., Brown, E., Duarte, C., 2014. The movement ecology of seagrasses. Proc. R. Soc. B: Biol. Sci. 281 (1795), 20140878. https://doi.org/10.1098/rspb.2014.0878.

Monismith, S.G., 2007. Hydrodynamics of Coral Reefs. Annu Rev. Fluid. Mech. 39 (1), 37–55. https://doi.org/10.1146/annurev.fluid.38.050304.092125.

Monismith, S.G., Hirsh, H., Batista, N., Francis, H., Egan, G., Dunbar, R.B., 2019. Flow and drag in a seagrass bed. J. Geophys. Res.: Oceans 124 (3), 2153–2163. https://doi.org/10.1029/2018JC014862.

Pastor, A., Catalán, I.A., Terrados, J., Mourre, B., Ospina-Alvarez, A., 2023. Connectivity-based approach to guide conservation and restoration of seagrass Posidonia oceanica in the NW Mediterranean. Biol. Conserv 285, 110248. https://doi.org/10.1016/j.biocon.2023.110248.

Peniston, J.H., Backus, G.A., Baskett, M.L., Fletcher, R.J., Holt, R.D., 2024. Ecological and evolutionary consequences of temporal variation in dispersal. Ecography. 2024 (2), e06699. https://doi.org/10.1111/ecog.06699.

Ramirez-Romero, E., Amores, A., Diaz, D., Muñoz, A., Catalan, I.A., Molinero, J.C., Ospina-Alvarez, A., 2023. Atmospheric–ocean coupling drives prevailing and synchronic dispersal patterns of marine species with long pelagic durations. Sci. Rep. 13 (1), 2366. https://doi.org/10.1038/s41598-023-29543-7.

Ruiz-Montoya, L., Lowe, R.J., Kendrick, G.A., 2015. Contemporary connectivity is sustained by wind- and current-driven seed dispersal among seagrass meadows. Mov. Ecol. 3 (1), 9. https://doi.org/10.1186/s40462-015-0034-9.

Ruocco, M., Lacorata, G., Palatella, L., Provera, I., Zenone, A., Martinez, M., Dattolo, E., Pazzaglia, J., Giacalone, V.M., Badalamenti, F., Procaccini, G., 2025. Movement ecology of a coastal foundation seagrass species: insights from genetic data and oceanographic modelling. Divers. (Basel) Distrib. 31 (2), e13944. https://doi.org/10.1111/ddi.13944.

Saint-Amand, A., 2022. Bridg. gap between small large spat. scales mar. dispersal model.: appl. coral ecosyst. Gt. Barrier Reef UCLouvain]. http://hdl.handle.net/2078.1/266081.

Saint-Amand, A., Lambrechts, J., Hanert, E., 2023a. Biophysical models resolution affects coral connectivity estimates. Sci. Rep. 13 (1), 9414. https://doi.org/10.1038/s41598-023-36158-5.

Saint-Amand, A., Lambrechts, J., Thomas, C.J., Hanert, E., 2023b. How fine is fine enough? Effect of mesh resolution on hydrodynamic simulations in coral reef environments. Ocean Model. 186, 102254. https://doi.org/10.1016/j.ocemod.2023.102254.

Schlaefer, J., Carter, A., Choukroun, S., Coles, R., Critchell, K., Lambrechts, J., Rasheed, M., Tol, S., Grech, A., 2022. Marine plant dispersal and connectivity measures differ in their sensitivity to biophysical model parameters. Environ. Model. Softw. 149, 105313. https://doi.org/10.1016/j.envsoft.2022.105313.

Smagorinsky, J., 1963. General circulation experiments with the primitive equations: I. The basic experiment. Mon. Weather Rev. 91 (3), 99–164. https://doi.org/10.1175/1520-0493(1963)091<0099:GCEWTP>2.3.CO;2.

Smith, S.D., Banke, E.G., 1975. Variation of the sea surface drag coefficient with wind speed. Q. J. R. Meteorol. Soc. 101 (429), 665–673. https://doi.org/10.1002/qj.49710142920.

Smith, T.M., York, P.H., Broitman, B.R., Thiel, M., Hays, G.C., van Sebille, E., Putman, N. F., Macreadie, P.I., Sherman, C.D.H, 2018. Rare long-distance dispersal of a marine angiosperm across the Pacific Ocean. Glob. Ecol. Biogeogr. 27 (4), 487–496. https://doi.org/10.1111/geb.12713.

Spagnol, S., Wolanski, E., Deleersnijder, E., Brinkman, R., McAllister, F., Cushman-Roisin, B., Hanert, E., 2002. An error frequently made in the evaluation of advective transport in two-dimensional lagrangian models of advection-diffusion in coral reef waters. Mar. Ecol. Prog. Ser 235, 299–302. https://www.int-res.com/abstracts/meps/v235/p299-302/.

Swearer, S.E., Treml, E.A., Shima, J.S., 2019. Chapter 7 A review of biophysical models of marine larval dispersal. In: Oceanography and Marine Biology, 57. Taylor & Francis. http://library.oapen.org/handle/20.500.12657/24720.

Tesson, S.V.M., Edelaar, P., 2013. Dispersal in a changing world: opportunities, insights and challenges. Mov. Ecol. 1 (1), 10. https://doi.org/10.1186/2051-3933-1-10.

Thomas, C.J., Bridge, T.C.L., Figueiredo, J., Deleersnijder, E., Hanert, E., 2015. Connectivity between submerged and near-sea-surface coral reefs: can submerged reef populations act as refuges? Divers. (Basel) Distrib. 21 (10), 1254–1266. https://doi.org/10.1111/ddi.12360.

Tol, S.J., Carter, A., York, P.H., Grech, A., Situ, R., & Coles, R.G. (2024). Estimates of wind drift coefficient to inform biophysical models of seagrass dispersal in the Great Barrier Reef. In *Oceanographic Processes of Coral Reefs* (2nd ed.). https://www.taylorfrancis.com/chapters/edit/10.1201/9781003320425-15/estimates-wind-drift-coefficient-inform-biophysical-models-seagrass-dispersal-great-barrier-reef-samantha-tol-alexandra-carter-paul-york-alana-grech-rong-situ-robert-coles.

Travis, J.M.J., Delgado, M., Bocedi, G., Baguette, M., Bartoń, K., Bonte, D., Boulangeat, I., Hodgson, J.A., Kubisch, A., Penteriani, V., Saastamoinen, M., Stevens, V.M., Bullock, J.M., 2013. Dispersal and species' responses to climate change. Oikos. 122 (11), 1532–1540. https://doi.org/10.1111/j.1600-0706.2013.00399.x.

Unsworth, R.K.F., Collier, C.J., Waycott, M., McKenzie, L.J., Cullen-Unsworth, L.C., 2015. A framework for the resilience of seagrass ecosystems. Mar. Pollut. Bull. 100 (1), 34–46. https://doi.org/10.1016/j.marpolbul.2015.08.016.

Urban, M.C., Bocedi, G., Hendry, A.P., Mihoub, J.-B., Pe'er, G., Singer, A., Bridle, J.R., Crozier, L.G., De Meester, L., Godsoe, W., Gonzalez, A., Hellmann, J.J., Holt, R.D., Huth, A., Johst, K., Krug, C.B., Leadley, P.W., Palmer, S.C.F., Pantel, J.H., Travis, J. M.J., 2016. Improving the forecast for biodiversity under climate change. Science 353 (6304), aad8466. https://doi.org/10.1126/science.aad8466.

van Gennip, S.J., Popova, E.E., Yool, A., Pecl, G.T., Hobday, A.J., Sorte, C.J.B., 2017. Going with the flow: the role of ocean circulation in global marine ecosystems under a changing climate. Glob. Chang. Biol. 23 (7), 2602–2617. https://doi.org/10.1111/gcb.13586.

Wagey, B., 2015. Morphometric study on the leaf width of the seagrass, halodule in relation to density, exposure, light and temperature in the Central Visayas, Philippines. Asian J. Biodivers. 6. https://doi.org/10.7828/ajob.v6i1.694.

Waycott, M., McMahon, K., Mellors, J., Calladine, A., Kleine, D., 2004. A Guide to Tropical Seagrasses of the Indo-West Pacific, 72. James Cook University, Townsville pp.

Weatherall, E.J., Jackson, E.L., Hendry, R.A., Campbell, M.L., 2016. Quantifying the dispersal potential of seagrass vegetative fragments: a comparison of multiple subtropical species. Estuar. Coast. Shelf. Sci. 169, 207–215. https://doi.org/10.1016/j.ecss.2015.11.026.

Wilson, L.J., Fulton, C.J., Hogg, A.M., Joyce, K.E., Radford, B.T.M., Fraser, C.I., 2016. Climate-driven changes to ocean circulation and their inferred impacts on marine dispersal patterns. Glob. Ecol. Biogeogr. 25 (8), 923–939. https://doi.org/10.1111/geb.12456.

Wolanski, E., Kingsford, M., Lambrechts, J., Marmorino, G., 2024. The physical Oceanography of the Great Barrier Reef: a review. Oceanographic Processes of Coral Reefs, 2nd Edition ed, p. 26. https://www.taylorfrancis.com/chapters/edit/10.1201/9781003320425-3/physical-oceanography-great-barrier-reef-eric-wolanski-michael-kingsford-jonathan-lambrechts-george-marmorino.

York, P.H., Carter, A.B., Chartrand, K., Sankey, T., Wells, L., Rasheed, M.A., 2015. Dynamics of a deep-water seagrass population on the Great Barrier Reef: annual occurrence and response to a major dredging program. Sci. Rep. 5 (1), 13167. https://doi.org/10.1038/srep13167.